Dalton Transactions

ROYAL SOCIETY OF CHEMISTRY

PAPER

View Article Online
View Journal | View Issue

Cite this: *Dalton Trans.*, 2025, **54**, 4903

$La_2ZnGa_2S_6O$: a melilite-type transition metal oxysulfide achieving a well-balanced nonlinear optical behavior†

Jingjing Xu,[a] Yan Xiao,[b] Xiaowen Wu, *[a,c] Bingbing Zhang *[b] and Kui Wu *[a]

Received 29th December 2024,
Accepted 27th January 2025

DOI: 10.1039/d4dt03569k

rsc.li/dalton

A combination of multiple anions (S^{2-} and O^{2-}) was developed as an effective method for exploring new, excellent nonlinear optical (NLO) oxysulfides with adjustable properties based on the flexible anion (S/O) ratio in their structures. It should be noted that mixed melilite-type oxysulfides, containing both alkaline earth (Ae) and trivalent lanthanide (Ln) metals, exhibit natural noncentrosymmetric (NCS) and disordered structures, demonstrating good NLO properties. Herein, we introduced low-coordination ZnS_4 to replace high-coordination AeS_8 in La-based melilite, thereby breaking the initial disordered structure and leading to the formation of a $La_2ZnGa_2S_6O$ NLO material with an ordered structure. Property investigations showed that $La_2ZnGa_2S_6O$ achieved a well-balanced NLO behavior, with a wide optical bandgap (3.0 eV) and an ultra-strong phase-matching second harmonic generation (SHG) response (1.9 × $AgGaS_2$). Among the melilite-type transition-metal oxysulfides, $La_2ZnGa_2S_6O$ exhibited the largest powder SHG response, which was attributed to the synergetic contributions of LaS_7O, ZnS_4 and GaS_3O anionic groups, based on SHG-density analysis. This indicates that $La_2ZnGa_2S_6O$ is a potential NLO candidate for frequency conversion applications, and the combination of transition and lanthanide metals in its structure provides a feasible pathway to design new large SHG oxysulfides.

Introduction

IR NLO crystals are usually used for critical laser frequency conversion, a field that has been recognized for decades as having significant applications in laser guidance, non-invasive medical diagnostics, IR remote sensing, and long-distance laser communication.[1–7] Traditional IR-NLO crystals, such as $AgGaS_2$ (AGS), $AgGaSe_2$ (AGSe), and $ZnGeP_2$ (ZGP), suffer from intrinsic drawbacks, including low laser-induced damage thresholds (LIDTs) and strong two-photon absorption, which have urged the exploration of novel crystals with high comprehensive performance.[8,9] An outstanding IR NLO crystal should possess a large NLO effect, large NLO effect coefficient comparable to AGS, wide bandgap for high LIDTs, and simultaneously large birefringence for phase-matching ability. However, these key factors are mutually related and restricted, making it a great challenge to achieve the aforementioned balanced performances.[10–14]

Previous nonlinear research has demonstrated that constructing heteroanionic compounds by combining multiple anionic groups provides a new way to balancing the aforementioned contradictions in materials, such as oxysulfides, chalcohalides, and oxyhalides. In recent years, oxysulfides, as an excellent infrared nonlinear optical material system, have attracted significant research interest and are rapidly developing as star materials.[15–21] Research on oxysulfide IR NLO materials indicates that most can achieve the optimal balance between two crucial parameters: SHG response and bandgap. Moreover, in oxysulfide structures, mixed-anion functional building groups exhibit a larger degree of distortion than single-anion-formed groups, which further shows flexible regulatory ability on material performance.[22–27]

Compounds containing d^{10} transition-metal cations (Zn^{2+}, Cd^{2+}, *etc.*) are important candidates for noncentrosymmetry (NCS) crystals because they exhibit a polar displacement of the d^{10}-cation center. Based on their electronic structural properties, transition metals maintain a large bandgap while increasing the frequency doubling effect of the material, making them suitable for designing nonlinear optical (NLO) materials.[28–31]

[a]*State Key Laboratory of Crystal Materials and Institute of Crystal Materials, Shandong University, Jinan 250100, China. E-mail: wukui@sdu.edu.cn*
[b]*College of Chemistry and Materials Science, Hebei University, Baoding 071002, China. E-mail: zhangbb@hbu.edu.cn*
[c]*School of Resources and Environment Engineering, Shandong Agriculture and Engineering University, School of Resources and Environment Engineering, Shandong Agriculture and Engineering University, China. E-mail: wuxiaowen1114@163.com*

†Electronic supplementary information (ESI) available. CCDC 2413312. For ESI and crystallographic data in CIF or other electronic format see DOI: https://doi.org/10.1039/d4dt03569k

In the vast library of inorganic nonlinear optical oxysulfide crystals, melilite-type compounds have been extensively studied. Most of them crystallize in the NCS space group $P\bar{4}2_1m$ with the general formula $A_2M^{I}N_2^{II}Q_7$. Among them, the M and N sites are mostly fourfold coordinated (Fig. S1†). Notably, tetrahedral anionic ligands are the most common structural motifs and always link together to form various structural types that have a significant effect on performance. Thus, the melilite system provides a large number of materials with an excellent balance of NLO properties.[32–40] Among them, melilite-type oxysulfides based on transition metals have been extensively studied and have demonstrated outstanding nonlinear optical properties (Fig. 1 and Table S1†).

In this study, we successfully synthesized another oxysulfide, $La_2ZnGa_2S_6O$, in the melilite system and investigated its performance characterization and theoretical calculations. The critical physicochemical properties of the title compound, including optical bandgap, Raman spectra, IR spectra, and powder SHG response, were systematically measured. The test results showed that it displayed the largest SHG response (1.9 × benchmark $AgGaS_2$ at a 38–55 μm particle size), a wide bandgap (3.0 eV), a wide IR transmission range and was non-hygroscopic. Moreover, property modulation with mixed anionic groups was also studied through theoretical calculations.

Results and discussion

The melilite-type oxysulfide $La_2ZnGa_2S_6O$ was found to crystallize in the NCS tetragonal space group $P\bar{4}2_1m$ (No. 113) with Z = 2 (Table S2†). Although it was reported in 1985,[41] its NLO properties have not been studied. Structurally, the asymmetric unit contained one La atom, one Zn atom, one Ga atom, one O atom and two S atoms. Both Zn and Ga were 4-fold coordinated with O/S atoms to form a tetrahedron. In contrast, Zn coordinated only with S atoms, while Ga formed bonds with one O and three S atoms (Fig. 2a). Two ZnS_4 and three GaS_3O units were connected with each other to form a $[Zn_2Ga_3S_{13}O_2]^{17-}$ five-membered ring (MR), and further, four 5-MRs were nested within each other to form a six-membered ring (Fig. 2b). The 5-MRs were arranged in parallel and connected to each other to form a two-dimensional (2D) layered structure (Fig. 2c); these layers were stacked along the c-axis with the La atoms situated within the interlayers (Fig. 2d). Up to now, reports on Ga-based mixed anion building blocks have mostly focused on the GaS_3O unit. Several oxysulfides, such as $LaGaS_2O$ [42] (GaS_2O_2); $[(Ba_{19}Cl_4)(Ga_6Si_{12}O_{42}S_8)]$ [43] (GaS_2O_2 and $GaSO_3$) $La_3Ga_3Ge_2O_{10}S_3$ [27] ($(Ga/Ge)S_2O_2$) and $Nd_3Ga_3Ge_2O_{10}S_3$ [6] (GaS_2O_2), contain other Ga-based mixed anion building blocks with different S:O ratios. As for the structure of $LaGaS_2O$, the GaS_2O_2 tetrahedral groups were interconnected to form a 1D chain structure extending along the a-axis (Fig. 2f). As shown in Fig. 2h, in $[(Ba_{19}Cl_4)(Ga_6Si_{12}O_{42}S_8)]$, two GaS_2O_2, four $GaSO_3$, and four $[Si_2O_7]^{6-}$ dimers apex-shared with each other to build a $[Si_8Ga_6O_{32}S_8]^{30-}$ circular cluster. The GaS_3O groups, similar to the title compound, were mostly connected by sharing O atoms to form clusters, such as dimers ($LaAeGa_3S_6O$ (Ae = Ca, Sr);[37] $Sr_5Ga_8O_3S_{14}$ [23]) or trimers ($Ga_9Tl_{13}O_2S_{13}$;[44] $K_2Ba_{0.5}Ga_9O_2S_{13}$ [45]). By comparing the structural analyses of the mixed anion groups with different S : O ratios, we found that the GaS_xO_{4-x} (x = 1, 2, and 3) mixed anion groups were

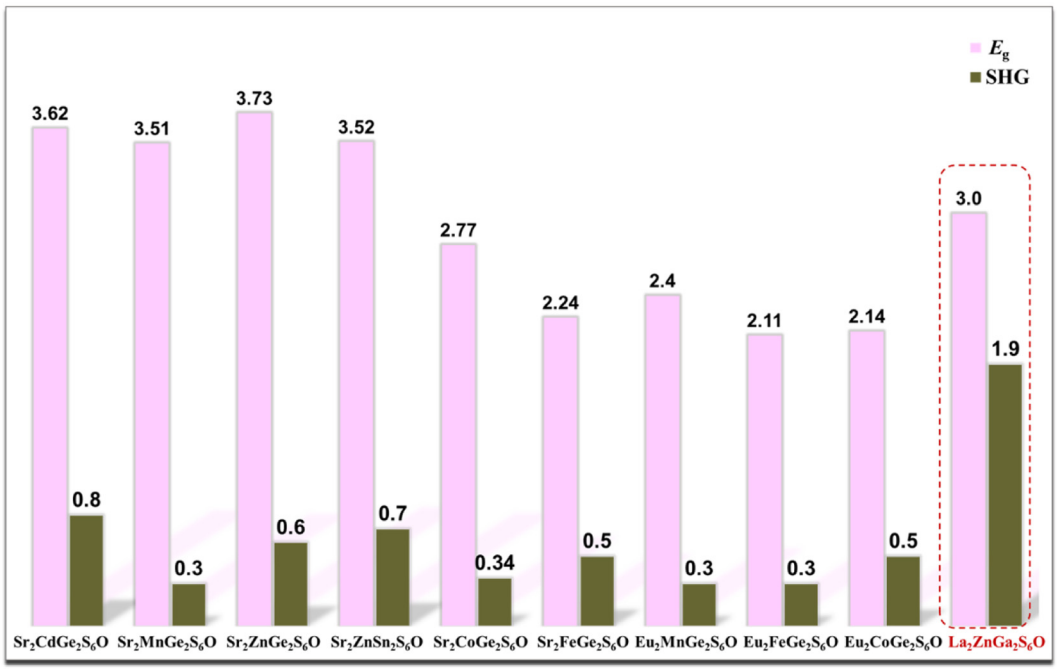

Fig. 1 Summary of the NLO properties of the reported melilite-type transition metal oxysulfides.

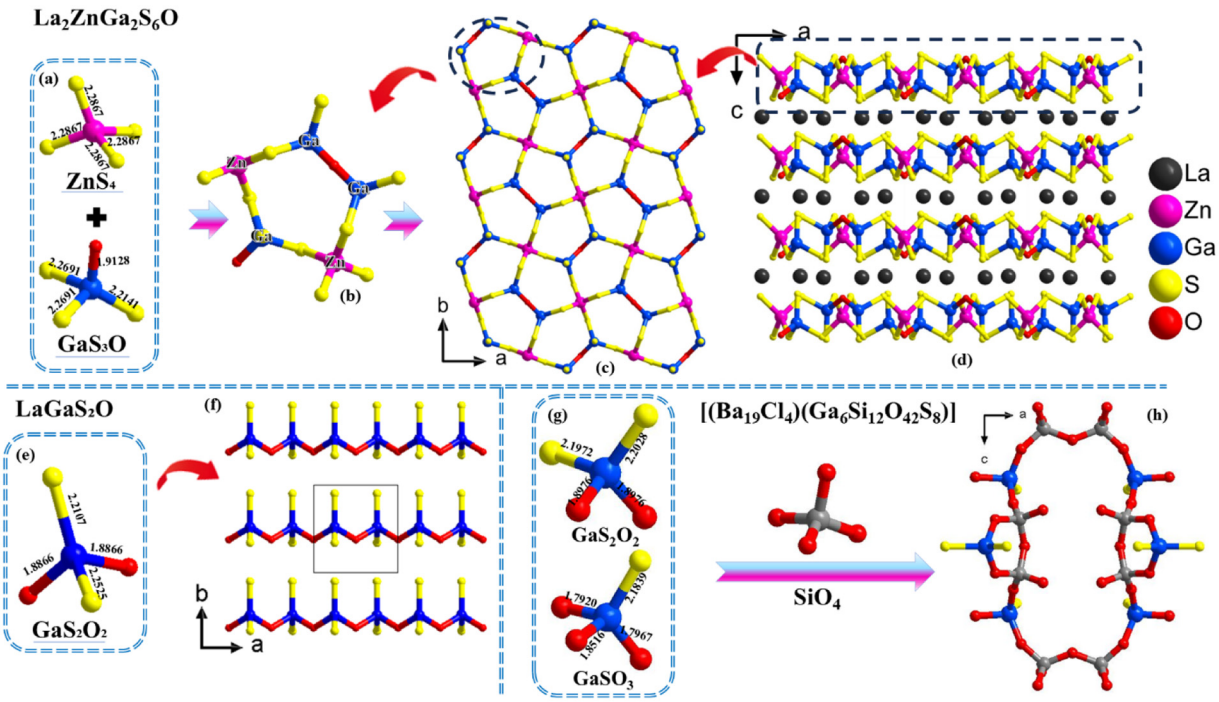

Fig. 2 (a) Coordination modes of the ZnS_4 and GaS_3O units; (b) $[Zn_2Ga_3S_{13}O_2]^{17-}$ five-membered ring; (c) 2D layer composed of ZnS_4 and GaS_3O units in $La_2ZnGa_2S_6O$; (d) crystal structure of $La_2ZnGa_2S_6O$ along the *b*-axis; (e) coordination modes of the GaS_2O_2 units; (f) 1D chain composed of GaS_2O_2 units in $LaGaS_2O$; (g) coordination modes of the $GaSO_3$ and GaS_2O_2 units; (h) $[Si_8Ga_6O_{32}S_8]^{30-}$ cluster formed by SiO_4, $GaSO_3$ and GaS_2O_2 BBUs.

more inclined to be connected by bridging O atoms to form 0D clusters or 1D chain-like structures.

The oxysulfide $La_2ZnGa_2S_6O$ was synthesized by a solid-state reaction in vacuum-sealed silica tubes. It was found to be stable in the air for several months. Powder X-ray diffraction (PXRD) tests showed that its experimental PXRD pattern was basically in agreement with the calculated one (Fig. 3a). We systematically studied the optical properties, including the bandgap, Raman spectra, and SHG response. Fig. 3b shows the UV-vis diffuse-reflectance spectra of $La_2ZnGa_2S_6O$, with a bandgap value of about 3.0 eV. To investigate the functional group-NLO property relationship of $La_2ZnGa_2S_6O$, a first-principles method was employed to perform the related theoretical calculations. Fig. 4a shows the result of the calculated bandgap, where it is clear that both the lowest conduction band (CB) and the highest valence band (VB) were located at the G points, indicating a direct bandgap of 2.48 eV. This value was smaller than the experimental result, which was ascribed to the unavoidable discontinuity of the exchange–correlation energy in the GGA calculation.

As for $La_2ZnGa_2S_6O$, the calculated partial density of states (PDOS) (Fig. 4b) showed that the valence band maximum (VBM: −5 to 0 eV) was composed of the S-3p and O-2p orbitals, and the PDOS near the bottom of the CB primarily consisted of the La-5d orbital, together with the minor S-3p orbital. Therefore, the charge transition between the CB and VB was determined by the LaS_7O units and had little relation to the Ga atoms.

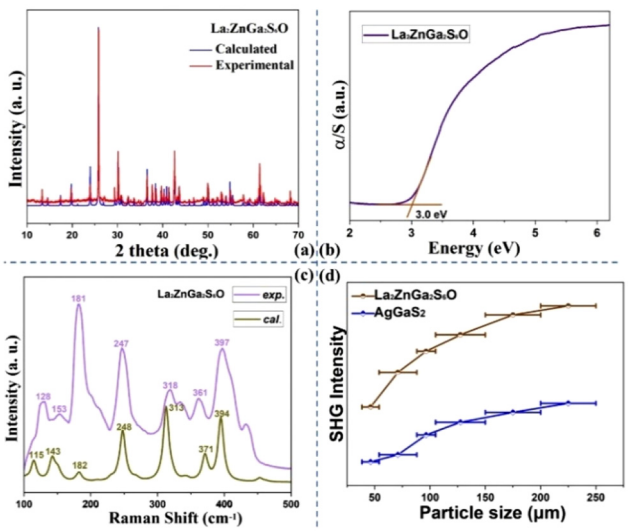

Fig. 3 (a) Experimental and calculated PXRD patterns for $La_2ZnGa_2S_6O$; (b) experimental optical bandgap for $La_2ZnGa_2S_6O$; (c) calculated and experimental Raman spectra for $La_2ZnGa_2S_6O$; (d) powder SHG response *versus* particle size for $La_2ZnGa_2S_6O$ with $AgGaS_2$ as the reference.

Raman spectra were measured and compared using experimental and theoretical calculations. The results showed excellent agreement between the experimental data and the simulated spectra. The measured Raman spectra exhibited no

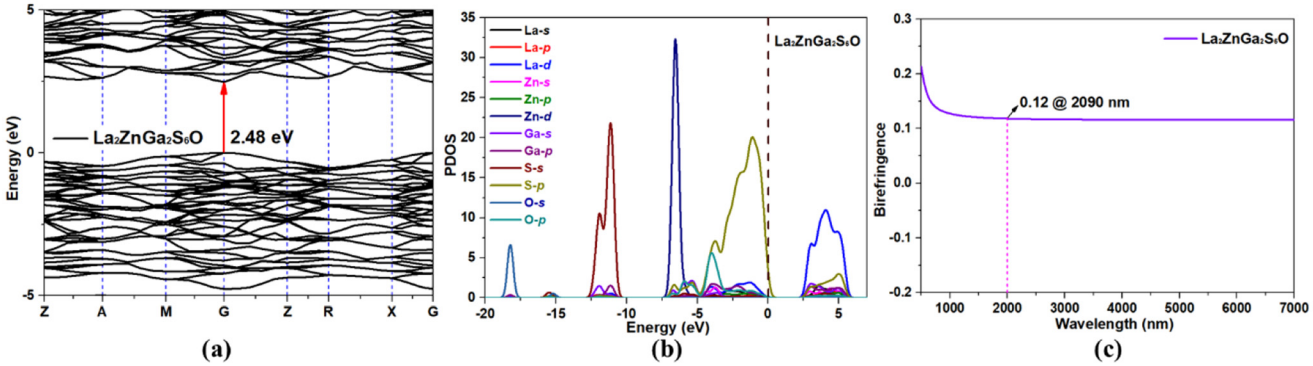

Fig. 4 (a) Band structure of $La_2ZnGa_2S_6O$; (b) PDOS of $La_2ZnGa_2S_6O$; (c) calculated birefringence of $La_2ZnGa_2S_6O$.

obvious absorption peaks in the wavenumber range from 500 to 4000 cm^{-1}, indicating a wide IR transmission range (18–20 μm) (Fig. 3c). Several Raman peaks located at 300–500 cm^{-1} were attributed to the Ga–S bond interaction, such as 318, 362, 397, and 433 cm^{-1}. Other peaks located at 200–300 cm^{-1} corresponded to the Zn–S bond vibration, which were similar to those of the previously reported Li_2ZnGeS_4 (260 cm^{-1}),[46] $Na_2ZnGe_2S_6$ (294 cm^{-1})[47] and $Sr_2ZnSn_2OS_6$ (272 cm^{-1}).[33] Moreover, the calculated IR spectra clearly show that there were no obvious absorption peaks in the range from 4000 to 550 cm^{-1}, indicating that $La_2ZnGa_2S_6O$ exhibited a wide IR transmission region up to 18 μm (550 cm^{-1}) (Fig. S2†). Using the typical Kurtz–Perry method, we investigated the powder SHG responses of the title compound with different particle sizes under 2.09 μm laser radiation, and the as-synthesized $AgGaS_2$ crystal was selected as the reference. The signal intensities showed a strengthening trend with the increase in particle size for the polycrystalline sample of $La_2ZnGa_2S_6O$, indicating phase-matching (PM) behavior (Fig. 3d). The title oxysulfide showed a good powder SHG response, about 1.9 times that of $AgGaS_2$, at the maximum 200–250 μm particle size. SHG-density calculation provided an intuitive understanding of the origin of the NLO effect, and the results showed that their NLO origin was derived from the synergistic effect between the LaS_7O, ZnS_4 and GaS_3O anionic groups (Fig. 5). Generally, birefringence, as a critical parameter, can be used to estimate the phase-matching capability. Herein, we also calculated the birefringence *versus* wavelength curves, and the birefringence (Δn) was found to be 0.12 at 2.09 μm, which was consistent with the phase-matching ability of the oxysulfide phase (Fig. 4c).

Moreover, by calculating and analyzing the distortion degree, we found that the distortion degree of the rare-earth metal coordination polyhedron was greater than that of the alkali earth metal coordination polyhedron, which also explains why the birefringence of the title compound is greater than that of the isomorphic alkaline-earth-metal-based compound $Sr_2ZnGe_2S_6O$ (Δn = 0.114) (Table S3†). Additionally, alkaline earth metals usually make relatively weak contributions to the SHG response, while rare-earth metals have certain advantages in expanding the SHG response.

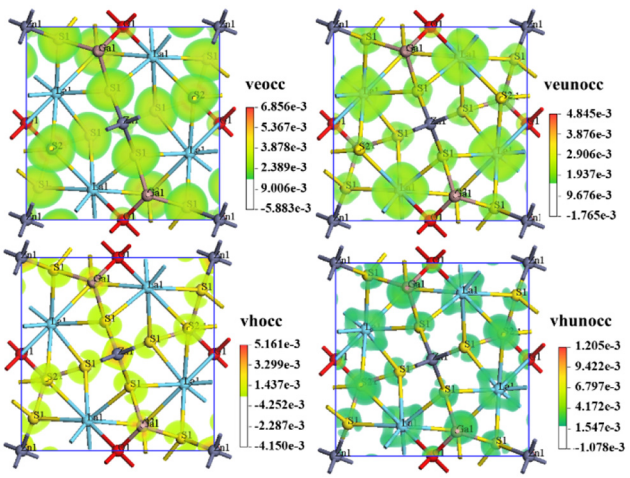

Fig. 5 Calculated SHG-density diagrams for the occupied and unoccupied states of $La_2ZnGa_2S_6O$.

Consequently, owing to the combined modulation effect of rare-earth metals and transition metals on SHG, the title compound demonstrated a relatively strong SHG response.

Conclusions

In summary, $La_2ZnGa_2S_6O$, a promising IR NLO oxysulfide material, was successfully synthesized using a high-temperature solid-state reaction. The title compound exhibited well-balanced nonlinear optical behavior and showed great potential as an NLO candidate material in the infrared frequency conversion field, with a wide bandgap (3.0 eV), strong SHG response (1.9 × AGS) and wide IR transmission range. Moreover, $La_2ZnGa_2S_6O$ exhibited the largest powder SHG response among the melilite-type transition-metal oxysulfides. Theoretical analysis showed that the synergistic regulation of ZnS_4, GaS_3O and LaS_7O contributed to the large SHG of the compound. The experimental and calculated results imply that lanthanide metals and transition metal tetrahedra can be used in the design of new large SHG oxysulfide materials.

Data availability

The authors confirm that the data supporting the findings of this study are available within the article and its ESI.†

Conflicts of interest

There are no conflicts to declare.

Acknowledgements

This work was supported by the National Natural Science Foundation of China (Grant No. 52372009 and 52402010), the open project of the Key Laboratory of Crystal Materials, Shandong University (KF2309) and the Qilu Young Scholar Program of Shandong University.

References

1 Y. Zhang, J. Chen, K. Li, H. Wu, Z. Hu, J. Wang, Y. Wu and H. Yu, *Nat. Commun.*, 2024, **15**, 2959.
2 Q. Q. Liu, X. Liu, M. Z. Li, R. X. Wang, B. Li, L. M. Wu and L. Chen, *Angew. Chem., Int. Ed.*, 2024, e202415318.
3 W. Xing, J. Tang, F. Liang, C. Tang, J. Wu, W. Yin, B. Kang and J. Deng, *Dalton Trans.*, 2023, **52**, 6915–6921.
4 H. Wang, X. Pan, S. Pan and J. Li, *Inorg. Chem. Front.*, 2024, **11**, 6919–6927.
5 K. Maeda, F. Takeiri, G. Kobayashi, S. Matsuishi, H. Ogino, S. Ida, T. Mori, Y. Uchimoto, S. Tanabe, T. Hasegawa, N. Imanaka and H. Kageyama, *Bull. Chem. Soc. Jpn.*, 2022, **95**, 26–37.
6 M. S. Zhang, B. W. Liu, X. M. Jiang and G. C. Guo, *Small*, 2023, **19**, 2302088.
7 W. Zhou and S.-P. Guo, *Acc. Chem. Res.*, 2024, **57**, 648–660.
8 A. Okorogu, S. Mirov, W. Lee, D. Crouthamel, N. Jenkins, A. Y. Dergachev, K. Vodopyanov and V. V. Badikov, *Opt. Commun.*, 1998, **155**, 307–312.
9 G. Boyd, E. Buehler and F. G. Storz, *Appl. Phys. Lett.*, 1971, **18**, 301–304.
10 V. G. Dmitriev, G. G. Gurzadyan and D. N. Nikogosyan, *Handbook of nonlinear optical crystals*, Springer, 2013.
11 G. D. Boyd, E. Buehler and F. G. Storz, *Appl. Phys. Lett.*, 1971, **18**, 301–304.
12 H. Chen, M.-Y. Ran, W.-B. Wei, X.-T. Wu, H. Lin and Q.-L. Zhu, *Coord. Chem. Rev.*, 2022, **470**, 214706.
13 X.-Y. Lou, Y. Zhou, W.-F. Chen, X.-M. Jiang, B.-W. Liu and G.-C. Guo, *Dalton Trans.*, 2023, **52**, 4873–4879.
14 Y.-F. Shi, W.-B. Wei, X.-T. Wu, H. Lin and Q.-L. Zhu, *Dalton Trans.*, 2021, **50**, 4112–4118.
15 Y. Zhang, H. Wu, Z. Hu and H. Yu, *Chem. – Eur. J.*, 2023, **29**, e202203597.
16 C. Larquet and S. Carenco, *Front. Chem.*, 2020, **8**, 179.
17 S. Cui, H. Wu, Z. Hu, J. Wang, Y. Wu and H. Yu, *Adv. Sci.*, 2022, **10**, 2204755.
18 S.-H. Zhou, M.-Y. Ran, W.-B. Wei, A. Y. Wang, X.-T. Wu, H. Lin and Q.-L. Zhu, *Inorg. Chem. Front.*, 2023, **10**, 5997–6004.
19 S. Cui, H. Wu, X. Dong, Z. Hu, J. Wang, Y. Wu, K. R. Poeppelmeier and H. Yu, *Adv. Sci.*, 2023, **11**, 2306825.
20 B. Almoussawi, W.-D. Yao, S.-P. Guo, M.-H. Whangbo, V. Dupray, S. Clevers, S. Deng and H. Kabbour, *Chem. Mater.*, 2022, **34**, 4375–4383.
21 Z. Li, S. Zhang, W. Xing, Z. Lin, J. Yao and Y. Wu, *Dalton Trans.*, 2020, **49**, 3667–3671.
22 X. Zhang, Y. Xiao, R. Wang, P. Fu, C. Zheng and F. Huang, *Dalton Trans.*, 2019, **48**, 14662–14668.
23 R. Wang, Y. Guo, X. Zhang, Y. Xiao, J. Yao and F. Huang, *Inorg. Chem.*, 2020, **59**, 9944–9950.
24 R. Wang, F. Liang, F. Wang, Y. Guo, X. Zhang, Y. Xiao, K. Bu, Z. Lin, J. Yao, T. Zhai and F. Huang, *Angew. Chem., Int. Ed.*, 2019, **58**, 8078–8081.
25 M. Y. Ran, S. H. Zhou, W. B. Wei, B. X. Li, X. T. Wu, H. Lin and Q. L. Zhu, *Small*, 2023, **19**, 2300248.
26 X. Zhang, L. Kang, P. Gong, Z. Lin and Y. Wu, *Angew. Chem., Int. Ed.*, 2021, **60**, 6386–6390.
27 H. Yan, Y. Matsushita, K. Yamaura and Y. Tsujimoto, *Angew. Chem., Int. Ed.*, 2021, **60**, 26561–26565.
28 H. Chen, W.-B. Wei, H. Lin and X.-T. Wu, *Coord. Chem. Rev.*, 2021, **448**, 214154.
29 Q. Q. Liu, X. Liu, L. M. Wu and L. Chen, *Angew. Chem., Int. Ed.*, 2022, **61**, e202205587.
30 G. Li, K. Wu, Q. Liu, Z. Yang and S. Pan, *Sci. China: Technol. Sci.*, 2017, **60**, 1465–1472.
31 L.-Q. Yang, X.-M. Jiang, S.-M. Pei, W.-F. Chen, B.-W. Liu and G.-C. Guo, *ACS Appl. Mater.*, 2022, **14**, 4352–4359.
32 M.-Y. Ran, S.-H. Zhou, B. Li, W. Wei, X.-T. Wu, H. Lin and Q.-L. Zhu, *Chem. Mater.*, 2022, **34**, 3853–3861.
33 Y. Cheng, H. Wu, H. Yu, Z. Hu, J. Wang and Y. Wu, *Chem. Sci.*, 2022, **13**, 5305–5310.
34 N. Zhang, Q.-T. Xu, Z.-H. Shi, M. Yang and S.-P. Guo, *Inorg. Chem.*, 2022, **61**, 17002–17006.
35 H.-D. Yang, S.-H. Zhou, M.-Y. Ran, X.-T. Wu, H. Lin and Q.-L. Zhu, *Inorg. Chem. Front.*, 2023, **10**, 2030–2038.
36 N. Zhang, X. Huang, W.-D. Yao, Y. Chen, Z.-R. Pan, B. Li, W. Liu and S.-P. Guo, *Inorg. Chem.*, 2023, **62**, 16299–16303.
37 J. Xu, K. Wu, Y. Xiao, B. Zhang, H. Yu and H. Zhang, *ACS Appl. Mater.*, 2022, **14**, 37967–37974.
38 R. Wang, F. Liang, X. Liu, Y. Xiao, Q. Liu, X. Zhang, L.-M. Wu, L. Chen and F. Huang, *ACS Appl. Mater.*, 2022, **14**, 23645–23652.
39 F.-X. Tian, N. Zhang, W.-D. Yao, M.-Y. Li, H.-P. Xu, W. Liu, J. Zhu and S.-P. Guo, *Inorg. Chem.*, 2024, **63**, 21810–21815.
40 Y. Chi, H.-G. Xue and S.-P. Guo, *Dalton Trans.*, 2018, **47**, 13434–13441.
41 C. L. Teske, *Z. Anorg. Allg. Chem.*, 2004, **531**, 52–60.
42 K. Ogisu, A. Ishikawa, Y. Shimodaira, T. Takata, H. Kobayashi and K. Domen, *J. Phys. Chem. C*, 2008, **112**, 11978–11984.

43 Y.-F. Shi, X.-F. Li, Y.-X. Zhang, H. Lin, Z. Ma, L.-M. Wu, X.-T. Wu and Q.-L. Zhu, *Inorg. Chem.*, 2019, **58**, 6588–6592.
44 S. Jaulmes, M. Julien-Pouzol, J. Dugué, P. Laruelle and M. Guittard, *Acta Crystallogr., Sect. C: Struct. Chem.*, 1986, **42**, 1111–1113.
45 J. N. Li, X. H. Li, Y. X. Xu, W. Liu and S. P. Guo, *Chin. J. Chem.*, 2022, **40**, 2407–2414.
46 Y. Huang, K. Wu, J. Cheng, Y. Chu, Z. Yang and S. Pan, *Dalton Trans.*, 2019, **48**, 4484–4488.
47 G. Li, K. Wu, Q. Liu, Z. Yang and S. Pan, *J. Am. Chem. Soc.*, 2016, **138**, 7422–7428.